Journal of Drug Delivery Science and Technology 77 (2022) 103855

Contents lists available at ScienceDirect

Journal of Drug Delivery Science and Technology

journal homepage: www.elsevier.com/locate/jddst

Accelerated wound closure rate by hyaluronic acid release from coated PHBV electrospun fiber scaffolds

Łukasz Kaniuk [a], Krzysztof Berniak [a], Agata Lichawska-Cieślar [b], Jolanta Jura [b], Joanna E. Karbowniczek [a], Urszula Stachewicz [a,*]

[a] Faculty of Metals Engineering and Industrial Computer Science, AGH University of Science and Technology, Cracow, Poland
[b] Department of General Biochemistry, Faculty of Biochemistry, Biophysics and Biotechnology, Jagiellonian University, Cracow, Poland

ARTICLE INFO

Keywords:
Electrospinning
Hyaluronic acid
Keratinocytes
PHBV fibers
Wound healing

ABSTRACT

The enormous potential of electrospun polymer fibers allows for their development in the field of biomaterials for tissue engineering and wound healing. Electrospun fibers based on biodegradable polymers such as poly(3-hydroxybutyrate-*co*-3-hydroxyvalerate) (PHBV) are an ideal material for the production of a biocompatible cell scaffold supporting wound closure and skin regeneration. The aim of this research was to create a fibrous PHBV scaffold supporting the 3D environment for anchoring and proliferation of keratinocytes. Moreover, hyaluronic acid (HA) has been used as a coating on PHBV fibers to improve the wound closure processes. ATR-FTIR results indicated the presence of HA in the PHBV scaffolds and UV–Vis analysis confirmed the release of HA from the fibers over 24h test. Importantly, this release of HA increase keratinocyte activity as well their proliferation leading to accelerated wound closure rate in the scratch tests. The designed HA-coated PHBV scaffolds demonstrate the great potential of surface-modified electrospun polymer fibers for wound healing.

1. Introduction

The skin, as a multilayered tissue, plays an extremely important role in protecting the body against the harmful effects of pathogens and other external thermal or physical factors [1,2]. Moreover, it reduces transepidermal water loss and maintains skin homeostasis through keratinocyte differentiation, migration and *stratum corneum* formation [3,4]. All these aspects prompt research to improve and accelerate the process of wound healing, concerning parameters related with wound depth, type, stage and nature of tissue damage [1,5]. The entire physiology of wound closure covers as many as 24 stages of cellular changes occurring during the hemostasis, inflammatory, cell proliferation and maturation [6,7]. Therefore, it is extremely important to improve the quality of wound healing by developing a material supporting skin tissue regeneration. An ideal wound scaffold should ensure an adequate level of gas exchange and skin hydration, remove excess exudate, provide mechanical protection and thermal insulation, be non-toxic, non-allergic, do not adhere to the wound, minimize scarring and have antibacterial properties [2,8,9]. Research on dressings for wound treatment is still carried out, but so far it has not been possible to design a dressing that reflects the natural skin tissue. The classical approach of tissue reconstruction is based on tissue repair with support of the cellular scaffold [10,11]. Morphology, topography or surface chemistry of scaffolds can influence the behavior of cells and thus the process of rebuilding the entire tissue [12,13]. The scaffolds provide temporary support for the cells, but atrophy when cells begin to produce their own extracellular matrix (ECM), therefore its degradation should allow sufficient time to form new tissue [6,14]. Indeed, biodegradability is to avoid inflammation associated with the prolonged presence of a foreign material in the body [15,16]. Cell migration and proliferation, gas exchange and nutrient transport depend mostly on the porosity and pore size of the scaffold. In wound healing, it is essential to promote the adhesion and growth of skin cells (fibroblasts) and epidermis (keratinocytes) and provide structures for local administration of therapeutic agents released to the wound area speeding up regeneration processes.

The scaffolds are in the form of porous sponges or fibrous meshes [11,17], often based on electrospun fibers as they are able to biomimic ECM [18,19]. Especially beneficial is high surface to volume ratio that in case of drug delivery systems allows encapsulation or adsorption of active compounds promoting healing process [20] and allowing to incorporate them as biosensors [21]. Biodegradable polymers are widely studied to create fibrous scaffolds especially poly

* Corresponding author.
E-mail address: ustachew@agh.edu.pl (U. Stachewicz).

https://doi.org/10.1016/j.jddst.2022.103855
Received 14 July 2022; Received in revised form 22 September 2022; Accepted 2 October 2022
Available online 5 October 2022

(3-hydroxybutyrate-*co*-3-hydroxyvalerate) (PHBV), which is thermoplastic, aliphatic polyester of the polyhydroxyalkanoate (PHA) group [5,15]. The advantage of PHBV is that it minimizes the risk of inflammatory reactions in tissues, as its degradation products are components of human blood [22,23]. Overall, PHBV has been extensively researched for applications in skin tissue engineering as a promising material promoting skin regeneration [5,6]. Our previous studies showed a satisfactory cellular response of osteoblasts and fibroblasts [24] in contact with PHBV fibers. The mechanical properties of PHBV membranes indicated a generally weak mechanical performance and rather brittle behavior [25,26] but PHBV is resistant to hydrolytic degradation and requires enzymes that can break down the polymer into hydroxy acids blocks [15,27]. However, in this study we investigated PHBV scaffolds for skin regeneration with surface of fibers modification with hyaluronic acid (HA) to achieve effective and faster wound healing process. HA is a linear polyanionic polysaccharide that occurs naturally in all living organisms, maintains the appropriate level of tissue hydration [28,29]. Similarly, to PHBV, HA is non-toxic, does not cause allergic or inflammatory reactions in the body and is commonly used in medical products [28,30]. HA is widely used as hydrogels, cell culture scaffolds, as well as physicochemical drug carriers [31]. It has been proven to reduce nervous sensitivity, so it can be used as a natural pain killer [29,32] and also wound healing aid [28,33]. Therefore, the aim of this research study was to demonstrate the effect of prolongated HA release from 3D electrospun PHBV scaffolds in supporting the wound closure process and in providing an appropriate environment for the migration and growth of keratinocytes.

2. Materials and methods

2.1. Electrospinning and coatings

PHBV (M_w = 450,000 g mol^{-1}, Helian Polymers, The Netherlands) was dissolved in chloroform and *N*,*N*-dimethylformamide (DMF) solution (volume ratio 9:1) to produce smooth fibers, and to obtain porous fibers, dimethyl sulfoxide (DMSO) was added in a volume ratio 8:1:1 (chloroform: DMF: DMSO, all solvents from POCH, Poland). Both of them were prepared to obtain 8 wt% solutions, which were stirred for 4h with a constant speed of 1000 rpm and temperature T = 48 °C.

PHBV fibers were electrospun using the electrospinning equipment EC-DIG with the climate system (IME Technologies, The Netherlands) at T = 25 °C, RH = 40% for smooth and RH = 70% for porous fibers. The positive voltage of 17 kV was applied to the stainless needle (0.5 and 0.8 mm of inner and outer diameter, respectively), which was kept at a distance of 20 cm to the grounded collector and the polymer solution flow rate was 0.1 ml min^{-1}. All fibers were randomly deposited.

As received electrospun PHBV samples were immersed in the HA (Hyaluronic acid sodium salt from *Streptococcus equi*, M_w = ~1.5–1.8 × 10^3 kDa, Sigma Aldrich, UK) solution (2.5 mg/1 ml deionized water) and were shaken overnight (25 °C, 100 rpm, Shaker IKA KS 3000 IC Control, Germany). Next day, coated fibrous membranes were gently washed using deionized water and dried overnight at T = 30 °C in the oven (Memmert SNB300, Germany). For further studies 4 types of samples were used: unmodified electrospun smooth and porous fibers named as sPHBV and pPHBV, respectively and coated samples named as sPHBV + HA and pPHBV + HA.

2.2. Morphology and wettability of PHBV scaffolds

All samples were coated with 8 nm Au layer using the rotary pump sputter coater (Q150RS, Quorum Technologies, UK). SEM micrographs were performed using Phenom ProX G6 Desktop SEM (Thermo Scientific, Waltham, MA, USA) at the accelerated voltage of U = 10 kV (fiber samples) and SEM (Merlin Gemini II, Zeiss, Germany), at the accelerated voltage of U = 3 kV (fibers with fixed and dehydrated cells). Fiber diameters (D_f) and pore diameter on fibers were measured using ImageJ (ver. 1.53c, USA) from SEM micrographs, based on 100 measurements for each sample. The average values were calculated with the standard deviations and results were additionally presented in form of histograms.

The wettability of PHBV scaffolds were analyzed by static contact angle method by applying 3 μl droplets of deionized water (DI water, Spring 5 UV purification system, Hydrolab, Straszyn, Poland) at T = 24 °C and RH = 38%. The images of 10 droplets were taken within 4 s from the deposition using Canon EOS 700D camera with EF-S 60 mm f/2.8 Macro USM zoom lens. The contact angles were measured using ImageJ (ver. 1.53c, USA) and the average values were calculated from 20 measurements with the standard deviations.

2.3. Chemical characterization of PHBV fibers and HA release

The functional groups of PHBV and HA in fibrous mats were recorded on Nicolet iS5 FT-IR spectrophotometer (Thermo Scientific, Waltham, MA, USA), by ATR technique using the diamond crystal. During measurements, the spectra were 64 repeated over the wavenumber range 500–4000 cm^{-1}, with resolution 4 cm^{-1}. Reference samples were PHBV fibers and HA powder, separately.

HA-coated PHBV fibers and 2 ml of distilled water were added to the 24-well plate and incubated in a shaker (25 °C, 150 rpm). The released acid was collected from the samples in four repetitions at time points (1, 2, 4, 8, 12 and 24h) and examined with a UV–Vis spectrophotometer (UV/VIS Excellence UV7, Mettler Toledo, Columbus, OH, USA). HA was detected by spectrophotometric measurement in an ultraviolet (UV) absorption spectrum at 190–280 nm against a blank containing deionized water. HA content in the released supernatant was calculated from the dilution curve.

2.4. In vitro studies - cell morphology and proliferation assay

In vitro studies have been carried out on human immortalized keratinocytes (HaCaT cell line) [34]. This cell line has, similarly to normal human epidermal keratinocytes (NHEK), high differentiation potential, which is mostly attributed to constitutive and induced expression of keratins and other differentiation markers. Thus, HaCaT cells are widely used to model skin keratinocytes, as a good alternative to NHEK [35]. All PHBV scaffolds were sterilized with UV light before cell culture. The culture was conducted up to 7 days using Dulbecco's Modified Eagle Medium (DMEM, Biological Industries, US) supplemented with 10% addition of fetal bovine serum (FBS), 2% antibiotics (penicillin and streptomycin), 1% amino acids and 1% L-glutamine (all from Biological Industries, US). The culture was grown under standard conditions in 37 °C, 90% humidity and 5% of CO_2 in the incubator (INCO 108 med, Memmert, Germany). The condition of the cells was checked after 1, 3 and 7 days. For the proliferation test and assessment of cell morphology the seeding concentration was 2 × 10^4 cells per well.

Cells were fixed in 4% paraformaldehyde solution (Sigma Aldrich, UK) for 15 min at 23 °C. Next, cells were permeabilized with 0.1% Triton X-100 in PBS for 10 min and then incubated in blocking solution (3% of BSA in PBS) for 60 min, both at 23 °C. For staining actin filaments, cells were incubated for 60 min at 23 °C with Alexa Fluor™ 488 Phalloidin (Thermo Fisher, USA). Nuclear DNA was stained with DAPI (Millipore, Germany) for 30 min at 23 °C.

A confocal microscope (Zeiss LSM 900 Airyscan2 with ZEN 3.1 software, Germany) was used for imaging fixed cells using a lens Plan-Apochromat 40 × /1.3 Oil DIC (UV), with the following imaging parameters: excitation 405 nm and emission detection bands 410–570 nm for DAPI and excitation 488 nm and emission detection bands 500–550 nm for Alexa Fluor™ 488 coupled with Phalloidin. Images were processed using ImageJ software (1.53v, USA). The z-stacks were recorded with the 1.5 μm step.

Cell proliferation was evaluated using CellTiter-Blue® Assay (Promega, US) after 1, 3 and 7 days of cell incubation. The results of the

study were correlated with two control samples, i.e. tissue culture polystyrene plate (TCPS) and the other, the same TCPS well in which the cells were grown, but with 200 µl of HA addition to the culture medium. A double control sample made it possible to test whether even directly added an amount of HA would affect the cell culture. On each test day, the medium was replaced with 400 µm of fresh medium and 80 µm of CellTiter-Blue® reagent, and incubated for 4h in 37 °C. From each well, 100 µm of supernatant was transferred to a 96-well plate in quadruplicate and fluorescence was read at 560/590 nm using a GloMax® Discover System microplate reader (Promega, US). The value of proliferation is expressed as a percentage according to the formula below:

$$Cell\ viability\ (\%) = \frac{(S_x - S_{\ control})}{(S_{100\%} - S_{\ control})} \times 100\%$$

where S_x is the fluorescence of the sample, $S_{\ control}$ is the fluorescence of the medium and $S_{100\%}$ is the fluorescence of 100% reduced dye.

2.5. In vitro wound healing assay - scratch test

In vitro wound healing assay was performed using HaCaT cell line to evaluate the effect of HA release from PHBV fibrous samples on cell migration. Keratinocytes were seeded in 24-well cell culture plates at concentration of 8×10^4 cell per well and incubated in 37 °C, 90% humidity and 5% of CO_2 for 48h in INCO 108med (Memmert, Germany). Then, a vertical scratch was made using 200 mL sterile pipet tip in the middle of each well through the monolayer of cells. Next, the medium in all the wells was replaced and the sterilized fibrous samples were placed over the scratched area without the cell surface touch, as was shown in Fig. 1. In this study, 2 cell controls were also performed, similarly to proliferation studies i.e. TCPS and TCPS well with 200 µl of HA addition to the culture medium. Wound closure was observed at 0, 2, 4, 8, 12 and 24h from the time of scratch formation. Imaging was performed using an inverted optical microscope (Leica DMi1, Leica Microsystems, Germany) with an objective lens (Leica *N*-Plan, 5 × /0.12PHO, Leica Microsystems, Germany). Images were analyzed using Leica LAS X software. The scratch length for all samples was the same and amounted to 1.66 mm in the tested area. Wound closure rate was quantified by measuring the gap between the boundaries of a cell-free scratch and was calculated from the following formula:

$$Wound\ closure\ rate\ (\%) = \frac{(A_0 - A_t)}{A_0} \times 100\%$$

where A_0 is the wound area at 0h and A_t is the wound area at the appropriate time point.

2.6. Statistical analysis

Analysis of variance (one-way ANOVA followed by Tukey's post-hoc test) was used to determine the level of significance between the PHBV samples, the statistical significance was evaluated at $p < 0.05$ for cell viability and $p < 0.01$ for wound closure rate. The statistical analysis was performed in Origin (ver. 2019b, USA).

3. Results and discussion

3.1. Morphology and wettability of scaffolds

We manufactured two types of scaffolds with smooth and porous electrospun PHBV fibers, see Fig. 2. The porosity in the fibers was obtained by adding DMSO in a mixture of solvents and increasing the humidity in the electrospinning chamber to 70% [20]. In addition, the increase in humidity in the electrospinning chamber contributed to vapor-induced phase separation (VIPS). When, the polymer solution is exposed to a water vapor, phase separation occurs in the polymer solution as a result of the diffusion of the gas phase with the surface of the solution. Thus, the increase of humidity during electrospinning of PHBV cause the pore formation on produced fibers [36,37]. The average diameter of the smooth fibers was 2.24 ± 0.29 µm, compared to 2.79 ± 0.32 µm of porous fibers, see Table 1. The increased diameter of porous fibers comes from increased humidity and the addition of DMSO, which reduced the rate of evaporation of solvent from the polymer jet [38]. The adsorption of HA into sPHBV fiber have not changed their morphology, the fibers still had a smooth surface, and their average diameter increased (2.33 ± 0.22 µm), but not exceeding the standard deviation. Similarly, the morphology and surface porosity of fibers were not affected by adsorbed HA, but slight increase of fiber diameter reaching 2.88 ± 0.29 µm for pPHBV + HA sample was observed. Previous studies confirm that the average values of PHBV electrospun fibers with similar electrospinning parameters are on average 2–3 µm [24,39,40]. However, much larger differences may result from changes in the concentration of the polymeric solution [41,42], the applied voltage [41,43], or the distance from the collector [41,44]. Both the diameter and the surface morphology of the fibers did not change significantly in the case of the HA coatings. On the other hand, in the SEM micrographs (Fig. 2D and E), residual HA in the form of films between the fibers is visible.

The wetting properties of the smooth and porous PHBV fibers showed the hydrophobic nature of the surface, and their contact angle was 121.72 ± 4.14° and 116.30 ± 4.35°, respectively, for sPHBV and pPHBV (Table 1). The images of the water droplet on the PHBV membranes are presented in Fig. S1 in the Supplementary materials. On the other hand, the contact angle for the HA-coated fibers showed a

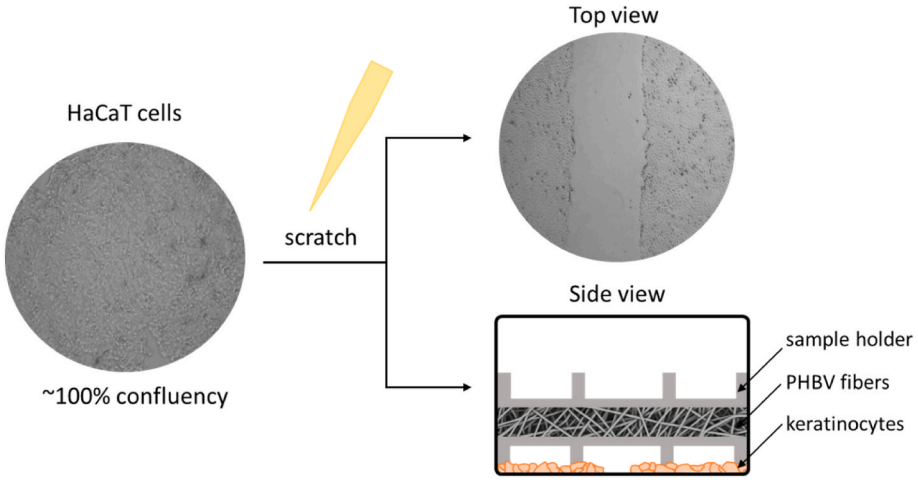

Fig. 1. Schematic illustration of scratch tests performed to verify the effect of using HA coating in PHBV scaffolds.

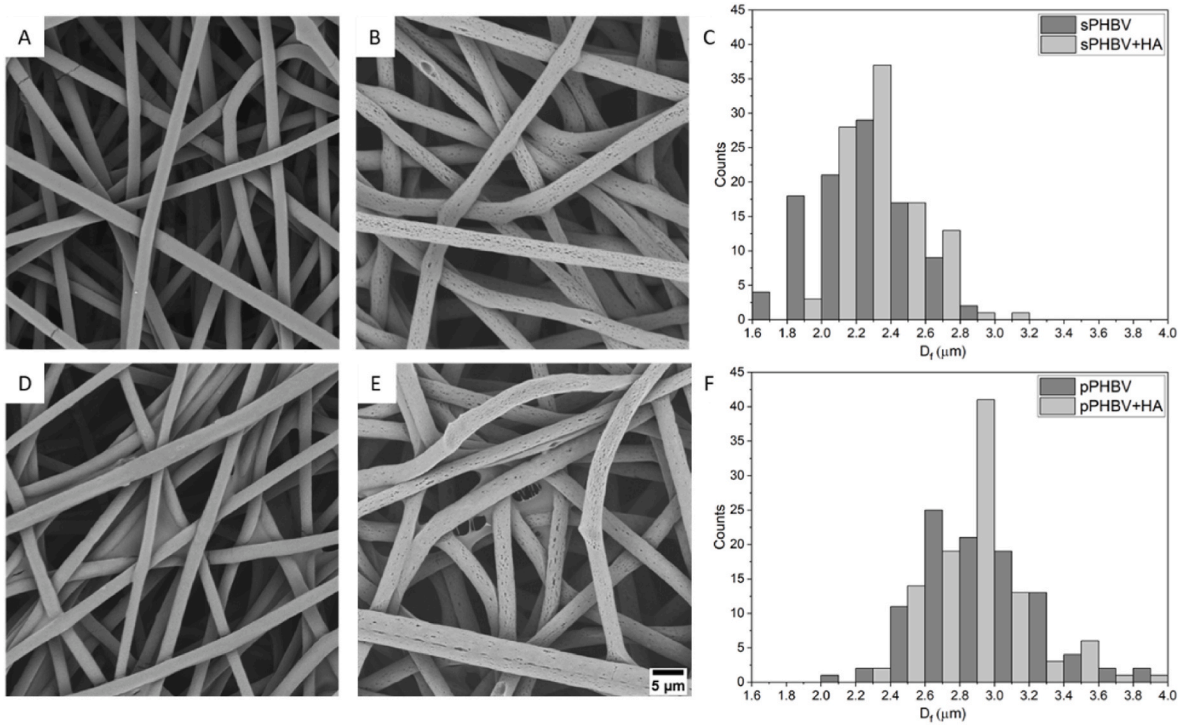

Fig. 2. SEM micrographs of the smooth (A, D) and porous PHBV fibers (B, E) and before (A, B) and after (D, E) HA coating, for all SEM images scale bar = 5 µm. Histograms of PHBV fiber diameter distribution before (C) and after (D) HA coating.

Table 1
The average diameters of PHBV electrospun fibers and the average water contact angles on PHBV mats.

	sPHBV	sPHBV + HA	pPHBV	pPHBV + HA
Average fiber diameter (µm)	2.24 ± 0.29	2.33 ± 0.22	2.79 ± 0.32	2.88 ± 0.29
Water contact angle (°)	121.72 ± 4.14	50.05 ± 2.49	116.30 ± 4.35	42.26 ± 2.53

significant change in wettability [45], to the hydrophilic character of the material. A slight decrease in the contact angle between smooth and porous PHBV fibers indicates a negligible effect of fibers porosity on the wetting of scaffolds. The decrease in the contact angle is often related to the surface roughness [46–48]. However, HA is highly hydrophilic and it is an excellent water adsorber [49–51]. Therefore, the coating of PHBV fibers with HA, changed their wetting profile to hydrophilic thus the lower contact angles are observed. However, for porous PHBV fibers the average surface pore size was 196.00 ± 99.21 nm, which fail to increase the roughness enough to change the wettability of scaffolds. Importantly, the HA coating does not block the pores in the fibers and scaffolds, as presented in Fig. 2.

3.2. Chemical characterization of PHBV fibers and hyaluronic acid release

Chemical analysis of electrospun fibers and HA was performed to confirm the presence of components and the complex of HA coated PHBV fibers. Fig. 3A presents the entire FTIR spectrum and the zoom region (Fig. 3B). The spectrum for PHBV fibers, both porous and smooth, shows the most intense absorption peak at about 1719 cm^{-1}, it is related to the C═O stretching vibration [26,40,52]. The characteristic absorption bands for PHBV related to the stretching vibrations of the C–H groups were observed in the area of 824–977 cm^{-1} and at 1228, 1260, 1275 and 2977 cm^{-1}, while the bending vibrations of the C–H groups were detected at 1377 and 1451 cm^{-1} [26,40,52]. Moreover, stretching bands of the C–O groups were noticed at 1053, 1097, 1128, and 1178 cm^{-1}. A band indicative of the $–CH_2–$ groups was indicated at 2931 cm^{-1} [26,40,52]. A broad band was observed for HA at 3660-3015 cm^{-1}, which is related to the stretching vibrations of the OH– and NH– groups [50,53]. An additional wide peak from the amides groups in HA is detected at the region 1700-1505 cm^{-1} and the stretching vibration of the α-glucopyranose structure (C–O–C groups) at 1020 cm^{-1} [54]. In the case of the coated PHBV fibers, there are visible bands from both HA, as the characteristic peaks at 1720 cm^{-1} of carbonyl groups and the $–CH_2–$ groups at 2930 cm^{-1} were spotted. The increasing absorbance on modified electrospun fibers spectrum are detected at characteristic HA ranges from OH– and NH– groups and amides groups, proving the presence of both compounds in the scaffolds.

Cumulative HA release profile from coated electrospun PHBV fibers are presented in Fig. 3C. Both modified fibers showed burst release approximately 60% during first hour of the test. An increase of the release is observed up to 4h. Then, the release profiles of HA were stabilized and achieve the cumulative release levels around 85% over 24h test. Similarly, HA release from coated electrospun poly(D,L-lactide) nanofibers in deionized water measured by Robertson et al. confirm the increased HA release during the first 5 h [50]. In case of PHBV the porosity of fibers allowed to incorporate and release slightly more HA, as it is indicted by the chemical analysis presented in Fig. 3.

3.3. Cell morphology and viability assay

In Fig. 4, the representative confocal images on different height from one field of selected planes show keratinocytes growth on the PHBV fibers after 7 days of cell incubation. Additionally, the confocal images of keratinocytes on PHBV fibers after 3 days of cell culture are included in Fig. S2 in the Supplementary materials. The stained actin enables to visualize the internal architecture of the cytoskeleton and the shape of cells growing on the samples. Importantly, the migration of cells after 7 days of incubation is very high. Keratinocytes growing on sPHBV fibers (Fig. 4A) formed a large agglomerate of cells, covering almost entire

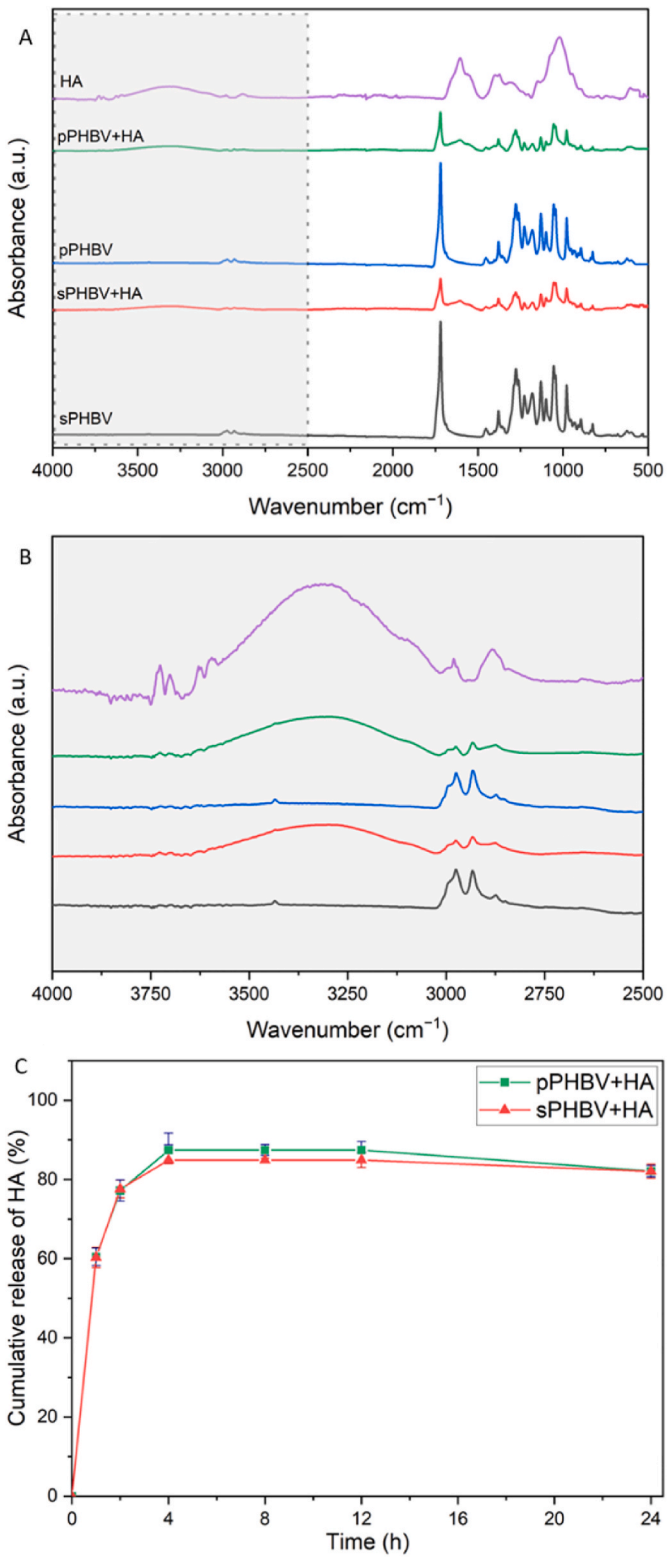

Fig. 3. The ATR–FTIR spectra of HA, smooth and porous PHBV fibers before and after HA coatings (A) and zoom for 4000-2500 cm^{-1} wavenumber region (B). Cumulative release profiles of HA from smooth and porous PHBV fibers over 24h (C).

scaffold. In the case of cells growing on coated sPHBV fibers, the actin cytoskeleton surrounding the polymer fibers is visible (Fig. 4B, Z = 0 μm). Deeper inside the sample structure, more and more cells are visible in the field of view, which indicates a large spread of cell colonies. Similar behavior was observed on porous PHBV samples. Keratinocytes formed large clusters on the pPHBV fibers throughout the scaffold cross-section (Fig. 4C), while on the coated pPHBV fibers, in the lowest imaged plane (Fig. 4B and D, Z = 0 μm), actin elongations on the fibers are visible. The obtained confocal images for all samples designate no significant differences in cell morphology between them.

Similar behavior of keratinocytes was observed on SEM micrographs in Fig. 5A–D after 7 days of cell culture. Images after 3 days of cell cultivation are included in Fig. S3 in the Supplementary materials. After 7 days in culture, the cells grow densely, and their elongation and migration are supported by the PHBV fiber network, which allows them to grow deeper into the scaffold structure. The random arrangement of the electrospun fibers indicates that cells migrate not only on top of them, but also deep down in the scaffolds. Importantly, cells are expanding in all possible directions, as long as the pore size allows them to migrate inside the 3D scaffolds [39,55,56]. Keratinocytes studies on the fibrous scaffold shows that cells can grow easily between the fibers as keratinocytes are relatively small cells in comparison to other types such as fibroblasts [57,58]. In Fig. 5A–D, the morphology of the formed cell clusters on PHBV fibers is a proof of high biocompatibility and indicating their growth and expansion [59]. We observed from both confocal and SEM imaging that proliferating keratinocytes are closely packed forming compact layer towards restoration of the skin protection. The PHBV scaffold structure facilitates cells overlapping to a depth of several micrometers allowing them to form a tight tissue.

Cell viability was determined with the CellTiter-Blue® Assay and the results show excellent cell proliferation, confirming the biocompatibility of all types of PHBV scaffolds (Fig. 5E). The results of the study were correlated with two control samples, which allows to check the direct effect of HA on the cell culture. The viability assay results presented a similar percentage of cell proliferation for all PHBV samples and controls on the 1st day of the experiment of approximately 15–20%. PHBV scaffolds after 1 day of cultivation showed statistically significant differences especially between control samples. On the 3rd day of culture, the proliferation of keratinocytes on unmodified and coated fibers was over 30%, with higher values for samples containing HA, while the TCPS controls were over 50%. However, on day 7, all samples reached cell proliferation over 90%. *In vitro* studies using keratinocytes confirm great proliferation on the PHBV scaffolds as well as other polyhydroxyalkanoate polymers [6,18]. Previous studies have shown that nanofiber membranes or nanoporous scaffolds support the proliferation of keratinocytes, due to increased adhesion of keratinocytes to the substrate [6,60]. The presented here research results prove that keratinocytes willingly proliferate also on microfibers, creating clusters and colonies of cells inside the porous scaffold between fibers. Additionally, almost 100% cell proliferation within 7 days of culture is unquestionable proof that both unmodified and HA-coated PHBV fibers are highly biocompatible and promote keratinocytes proliferation.

3.4. *In vitro* wound healing assay - scratch test

The effect of the HA release from PHBV scaffolds on the wound healing activity was investigated by an *in vitro* scratch test. The wound closure steps present the areas of wound healing, see Fig. 6 and Fig. S4 in Supplementary materials. After 2h from creating the scratch, the wound decreased by approximately 10%, which is visible as high cell numbers at the periphery of the scratch. Cells migrate and multiply along both scar edges of the created wound over time. Wound closure progressed over time; after 8h it was closed to 30% for TCPS and pPHBV + HA. In the case of the TCPS control with the HA additive in the medium, it was closed even more than 40%. After 12h, higher differences between the samples with and without the addition of HA was observed. It resulted in the wound closure rate 10% faster for HA coated PHBV scaffolds than pristine PHBV. After 24h, both TCPS with HA and PHBV fibers coated with HA showed complete closure of the wound, proving the accelerating effect of HA in wound healing process. The differences between

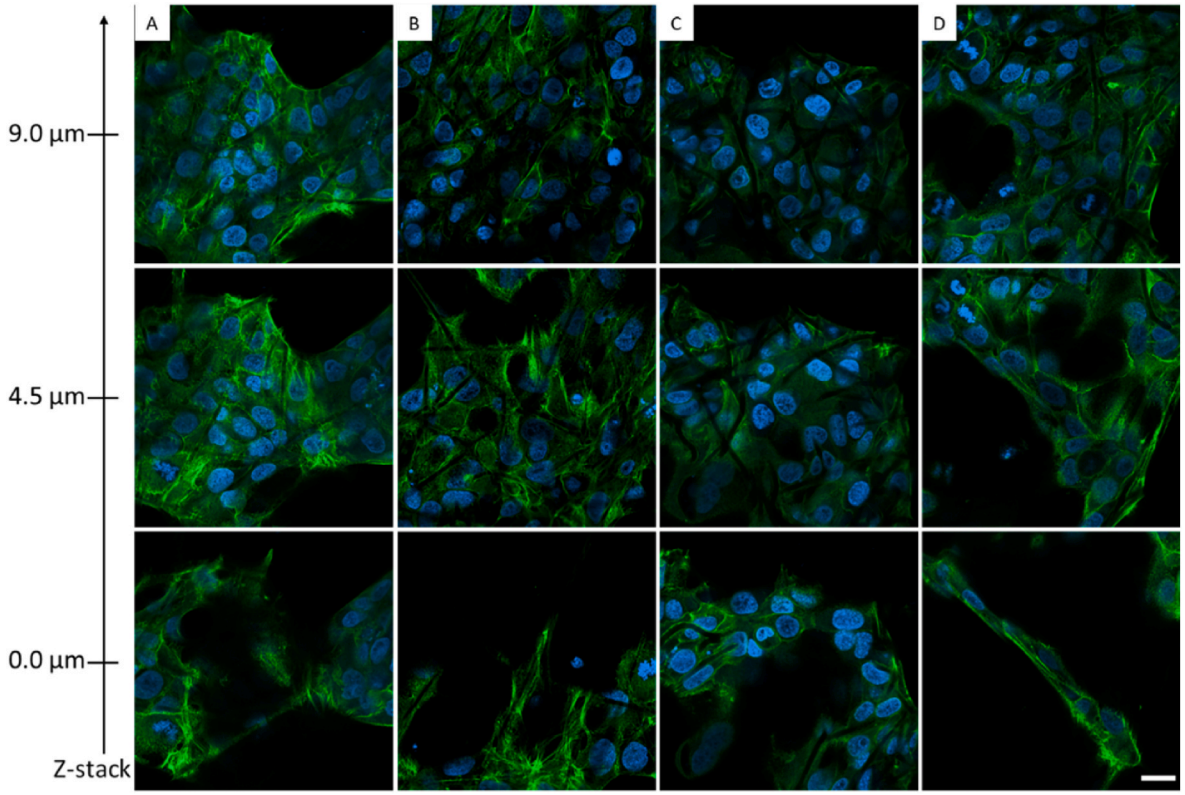

Fig. 4. Z-stacks (3 selected planes) of CLSM images of keratinocytes on unmodified PHBV fibers (A – smooth, C – porous) and coated with HA (B – smooth, D – porous) after 7 days of cell incubation. The nucleus was stained with DAPI (blue) and the actin fibers with Alexa Fluor™ 488 Phalloidin (green), for all images scale bar = 20 µm. (For interpretation of the references to colour in this figure legend, the reader is referred to the Web version of this article.)

smooth and porous PHBV fibers were negligible, however the increase of scratch shrinkage rate between the pristine PHBV fibers and coated with HA is directly corelated with HA release into the cell culture medium. It may suggest that obtained small porosity of PHBV fibers did not incorporate more HA and increased the release of HA during the scratch tests. It was confirmed with the HA release test presented in Fig. 3C. The cumulative amount of HA released confirms that approximately 80% of the HA is released from the coated PHBV scaffolds within 4h. We started to observe a stable level of HA release after 4h but wound closure rate speeds up after 8h, as it is presented in the chart showing the results from the scratch test in Fig. 6G.

Wound healing is a multi-phase and multi-stage process influenced by many external factors [61]. The process of cell migration to promote wound closure is critical in skin tissue regeneration and restoring its protective function. It has been proved that nanoparticles incorporated in fibers [55] or essential oils [61,62] improve the cell migration and increase the antibacterial activity. PHBV membranes containing cerium oxide nanoparticles have great potential as a wound dressing to enhance vascularization, and to aid diabetic wound healing [55]. In addition, studies of PHBV nanofiber dressings containing curcumin have shown that the use of a natural additive, curcumin, increased cell proliferation and may support the wound healing process [5]. Moreover, the extensive research has been conducted to evaluate PHBV and polydioxanone (PDX) electrospun scaffolds, which can biomimic the piezoelectric properties of biological tissues to promote their regeneration [63]. Physicochemical and piezoelectric properties supported stimulation, migration and proliferation of fibroblasts, reduced wound contraction and macrophage-induced inflammation, increased keratinocyte proliferation, and an overall balance between phenotypes of endothelial cells. *In vivo* studies confirmed that the wound healing was accelerated, as well as the reduction of fibrosis and scarring of the wound [63]. However, the previous studies lack combining electrospun PHBV fibers with HA, which we show here as a very effective fusion supporting wound closure. Importantly, HA offers numerous advantages in topical delivery for the treatment of skin conditions over systemic therapies. These assets include easy access to the skin, patients are more susceptible to local drug delivery, and also avoid hepatic metabolism [28]. HA can stimulate pro-inflammatory mediators, inhibiting the migration of leukocytes and macrophages [29,30,51]. It is applied in the treatment of arthritis as well as tissue repair, especially wound healing [30,33,51]. Moreover, HA is naturally present in high concentrations in the skin and soft connective tissues, therefore the use of HA is a suitable choice for supporting skin regeneration and augmentation [29]. It has been proven that HA as the main component of ECM, filling connective tissue, performs numerous biological functions related to the processes of angiogenesis, and inflammation, and can also be used as filling, in particular of cartilage tissue [31,64]. Also, the recent studies of injecting hydrogels into the sites of cartilage tissue have shown great potential for tissue regeneration [65]. Besides, the photopolymerizable HA hydrogels have been extensively studied in the regeneration of cartilage tissue by encapsulating various stem cells, which also affects the production of new tissue stem cells [31,66]. Hyaluronan as part of the ECM forms the basis for the organization of proteoglycans and forms connections with collagen, fibrin and other matrix molecules. In wound healing, the response to tissue damage involves the formation of a temporary matrix rich in hyaluronan and fibrin, which promotes the proliferation of fibroblasts and endothelial cells at the wound site, followed by the formation of granulation tissue. The hydrophilic nature of hyaluronan creates an environment that allows cells to migrate to the rebuilt tissue sites, while its antioxidant properties protect cells and ECM molecules against free radicals and proteolytic damage. This entire process mediates the healing of wounds, especially acute and chronic wounds [67]. Moreover, it has been proven that HA binds to a key transmembrane protein which role in the skin formation [68]. HA is also a regulator of

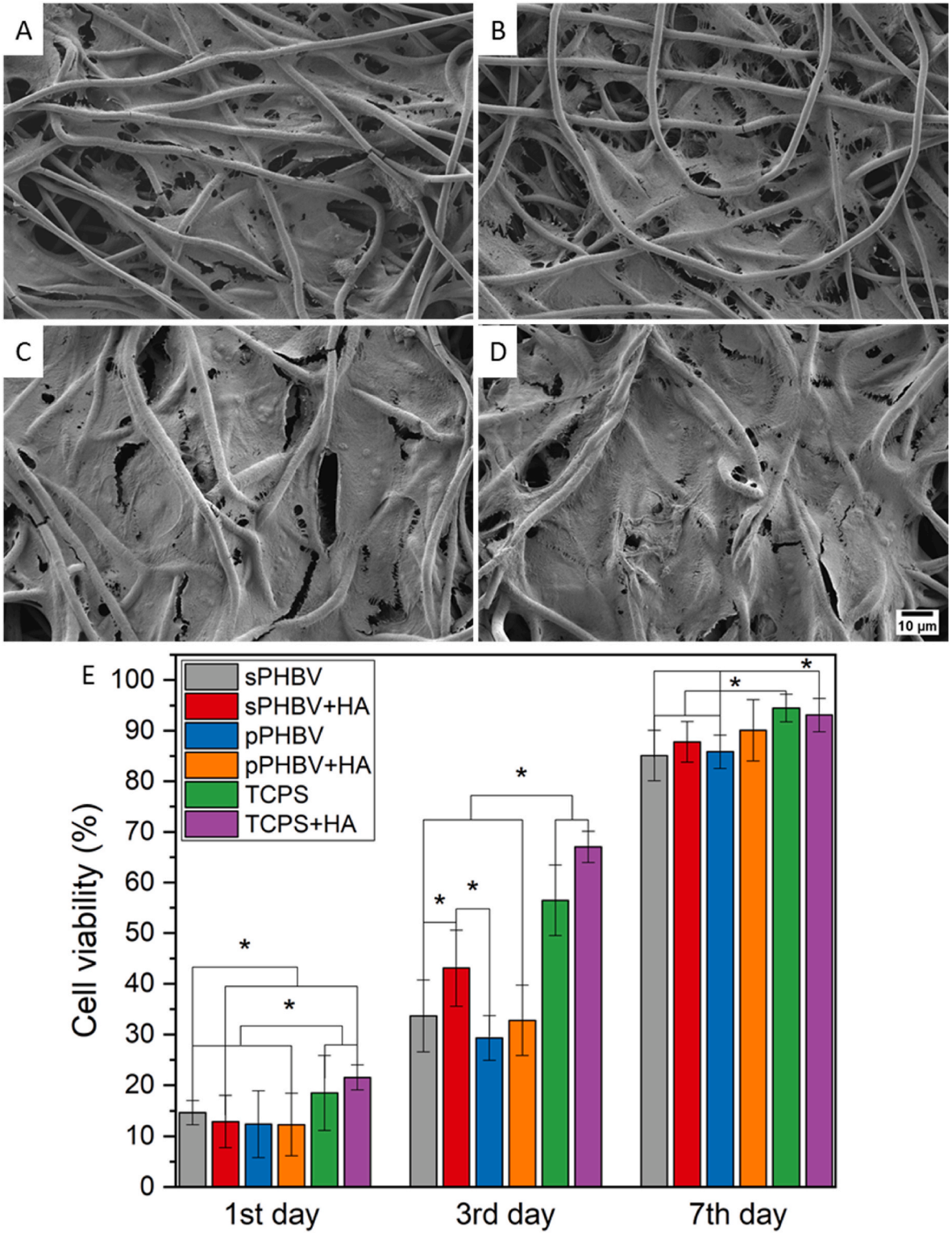

Fig. 5. SEM micrographs showing keratinocytes growth on unmodified PHBV fibers (A – smooth, C – porous) and coated with HA (B – smooth, D – porous) after 7 days of cell incubation. For all images scale bar = 10 µm. Cell viability based on CellTiter-Blue® (E). *statistical significance was evaluated at $p < 0.05$, using one-way ANOVA followed by Tukey's post-hoc test. (For interpretation of the references to colour in this figure legend, the reader is referred to the Web version of this article.)

cell behavior and has a significant impact on the processes of cell migration and proliferation. The presence of HA affects the local hydration of tissues and weakens the anchoring of cells in ECM, which facilitates their detachment, and thus their migration and cell division [49,67,69]. Moreover, HA binds to cells with surface receptors, e.g. CD44 and Receptor for HyaluronAn Mediated Motility (RHAMM), which can bind to protein kinases responsible for cell movement. CD44 is the main cell surface receptor for hyaluronan, the cellular interaction of which is related to cell adhesion and migration, their proliferation and activation, as well as the capture and degradation of hyaluronan. RHAMM is responsible for the locomotion of cells [54,67,69].

Therefore, HA is able to enhance cell proliferation and the results

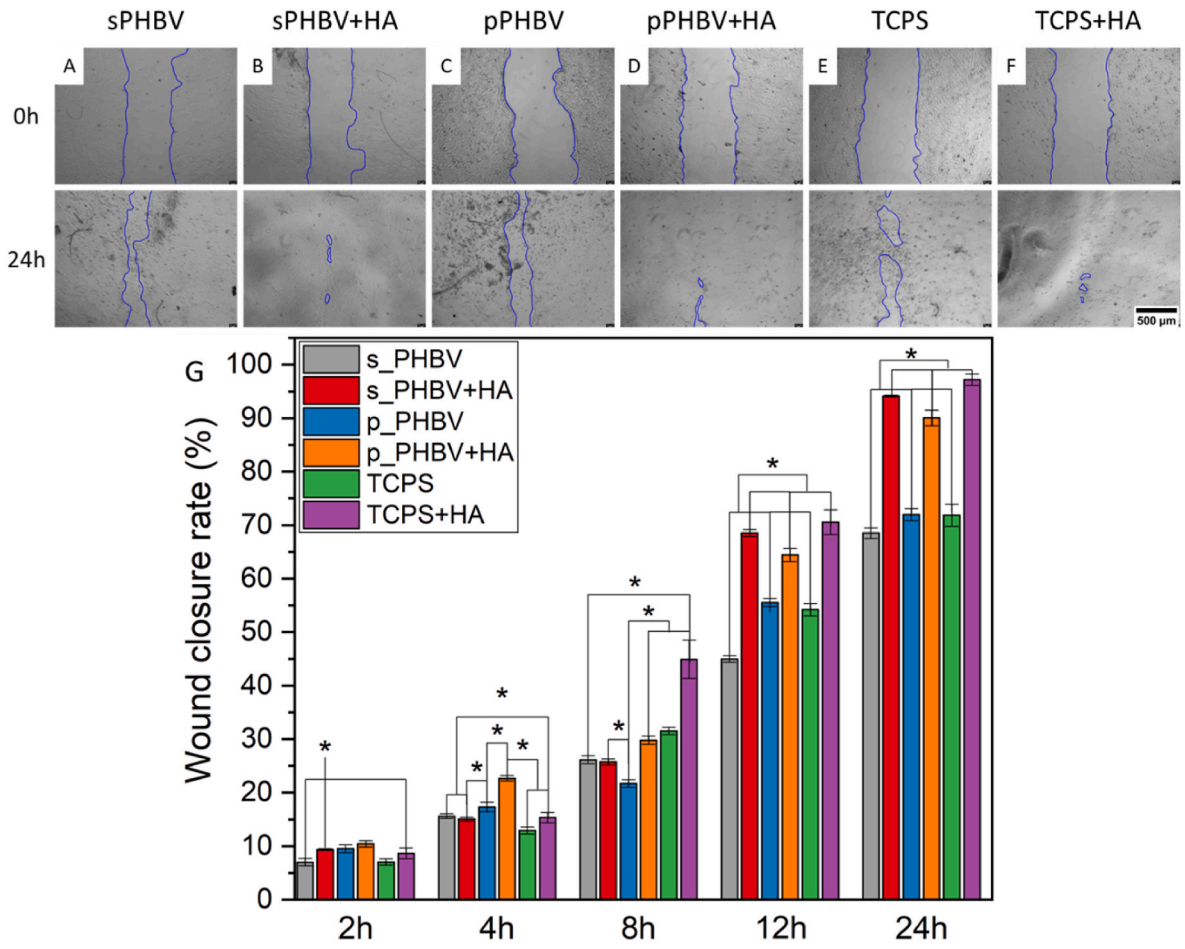

Fig. 6. Optical microscope images of wounded areas at 0h and after 24h of incubation (A–F), for all images scale bar = 500 µm. Wound closure rate at the time points (G), *statistical significance was evaluated at $p < 0.01$, using one-way ANOVA followed by Tukey's post-hoc test.

from *in vitro* scratch tests confirm that PHBV fibers with HA coating promote cell migration and wound healing. Previous studies focusing on the wound closure process were carried out only after 20 [55] or 6 and 24h [61]. Our research aimed at showing precisely the different stages of wound closure including 2, 4, 8, 12 and 24h steps. The intermediate scratch test times were used to evaluate wound closure, while clearly demonstrating that after just 12h the addition of HA accelerated wound closure. It allows us to corelate the standard release UV–Vis tests for HA from the 3D scaffolds to the effect of wound closer rate. Interestingly the delay in HA release does not show the wound closer rate reaching the same level as it happens in the control samples TCPS + HA. Keeping in mind that biodegradable PHBV fibers biomimic the natural 3D environment for cells, we created a unique system delivering HA and having a great potential in efficient wound healing.

4. Conclusions

Skin wound closer is still one of the major problems in regenerative medicine. In this study, we have shown that PHBV electrospun fibers can be effective in promoting keratinocyte proliferation. The epidermal cells satisfactorily migrated deep into the scaffolds, creating the 3D clusters of cells throughout the network of electrospun fibers. We successfully coated PHBV fibers with HA using the adsorption process. ATR-FTIR results indicated HA presence on PHBV fibers and the UV–Vis analysis confirmed the release of HA from the fibers over 24h. The delay of 4h HA release from scaffolds does not delay the wound closure rate. Moreover, the random electrospun fibers allowed for a natural reflection of the ECM structure, while HA influenced also biological factors such as increasing the proliferation and migration of keratinocytes. We provided the combination of 3D environment and HA release to increased significantly the wound closure rate. This research highlights the great need to support wound healing and the importance of cell-material interactions in this complex regeneration process. The designed tissue scaffold based on HA-coated PHBV fibers demonstrates the enormous potential of surface-modified electrospun polymer fibers for wound healing. The further studies will include the cytotoxicity and in vivo tests.

CRediT author statement

Łukasz Kaniuk: Conceptualization, Methodology, Validation, Formal analysis, Investigation, Data curation, Writing - original draft, Writing - review & editing, Visualization.

Krzysztof Berniak: Methodology, Validation, Investigation, Data curation, Writing - original draft, Writing - review & editing, Visualization.

Agata Lichawska-Cieślar: Methodology, Resources.

Jolanta Jura: Resources, Methodology.

Joanna E. Karbowniczek: Conceptualization, Validation, Data curation, Writing - original draft, Writing - review & editing, Supervision.

Urszula Stachewicz: Conceptualization, Methodology, Validation, Data curation, Writing - original draft, Writing - review & editing, Supervision, Project administration, Funding acquisition, Resources.

Declaration of competing interest

The authors declare that they have no known competing financial interests or personal relationships that could have appeared to influence the work reported in this paper.

Data availability

Data will be made available on request.

Acknowledgements

This research was part of the "Nanofiber-based sponges for atopic skin treatment'' project carried out within the First TEAM program of the Foundation for Polish Science co-financed by the European Union under the European Regional Development Fund, project No POIR.04.04.00-00-4571/17–00.

Appendix A. Supplementary data

Supplementary data to this article can be found online at https://doi.org/10.1016/j.jddst.2022.103855.

References

[1] J. Wang, M. Windbergs, Functional electrospun fibers for the treatment of human skin wounds, Eur. J. Pharm. Biopharm. 119 (2017) 283–299, https://doi.org/10.1016/j.ejpb.2017.07.001.
[2] I. Unalan, B. Slavik, A. Buettner, W.H. Goldmann, G. Frank, A.R. Boccaccini, Physical and antibacterial properties of peppermint essential oil loaded poly (ε-caprolactone) (PCL) electrospun fiber mats for wound healing, Front. Bioeng. Biotechnol. 7 (2019), https://doi.org/10.3389/fbioe.2019.00346.
[3] Z.W.K. Low, Z. Li, C. Owh, P.L. Chee, E. Ye, K. Dan, S.Y. Chan, D.J. Young, X.J. Loh, Recent innovations in artificial skin, Biomater. Sci. 8 (2020) 776–797, https://doi.org/10.1039/c9bm01445d.
[4] Y.J. Son, J.W. Tse, Y. Zhou, W. Mao, E.K.F. Yim, H.S. Yoo, Biomaterials and controlled release strategy for epithelial wound healing, Biomater. Sci. 7 (2019) 4444–4471, https://doi.org/10.1039/c9bm00456d.
[5] G. Mutlu, S. Calamak, K. Ulubayram, E. Guven, Curcumin-loaded electrospun PHBV nanofibers as potential wound-dressing material, J. Drug Deliv. Sci. Technol. 43 (2018) 185–193, https://doi.org/10.1016/j.jddst.2017.09.017.
[6] D. Sundaramurthi, U.M. Krishnan, S. Sethuraman, Biocompatibility of poly(3-hydroxybutyrate-co-3-hydroxyvalerate) (PHBV) nanofibers for skin tissue engineering, J. Biomed. Nanotechnol. 9 (2013) 1383–1392, https://doi.org/10.1166/jbn.2013.1618.
[7] P. Teller, T.K. White, The Physiology of Wound Healing: Injury through Maturation, vol. 89, Surgical Clinics of North America, 2009, pp. 599–610, https://doi.org/10.1016/j.suc.2009.03.006.
[8] J. Chen, J. Yang, L. Wang, X. Zhang, B.C. Heng, D.A. Wang, Z. Ge, Modified hyaluronic acid hydrogels with chemical groups that facilitate adhesion to host tissues enhance cartilage regeneration, Bioact. Mater. 6 (2021) 1689–1698, https://doi.org/10.1016/j.bioactmat.2020.11.020.
[9] M. Wójcik, A. Wilczyńska, V. Vivcharenko, P. Kazimierczak, Ł. Adaszek, A. Przekora, Bioactive Curdlan/Agarose dressing enriched with gentamicin for infected wounds - pilot studies, Eng. Biomater. 160 (2021) 2–7, https://doi.org/10.34821/eng.biomat.160.2021.2-7.
[10] B. Mammadov, M. Sever, M.O. Guler, A.B. Tekinay, Neural differentiation on synthetic scaffold materials, Biomater. Sci. 1 (2013) 1119–1137, https://doi.org/10.1039/c3bm60150a.
[11] Y. Chen, M. Shafiq, M. Liu, Y. Morsi, X. Mo, Advanced fabrication for electrospun three-dimensional nanofiber aerogels and scaffolds, Bioact. Mater. 5 (2020) 963–979, https://doi.org/10.1016/j.bioactmat.2020.06.023.
[12] T.P. Kunzler, T. Drobek, M. Schuler, N.D. Spencer, Systematic study of osteoblast and fibroblast response to roughness by means of surface-morphology gradients, Biomaterials 28 (2007) 2175–2182, https://doi.org/10.1016/j.biomaterials.2007.01.019.
[13] P. Kuppan, K.S. Vasanthan, D. Sundaramurthi, U.M. Krishnan, S. Sethuraman, Development of poly(3-hydroxybutyrate-co-3-hydroxyvalerate) fibers for skin tissue engineering: effects of topography, mechanical, and chemical stimuli, Biomacromolecules 12 (2011) 3156–3165, https://doi.org/10.1021/bm200618w.
[14] D. Sundaramurthi, K.S. Vasanthan, P. Kuppan, U.M. Krishnan, S. Sethuraman, Electrospun nanostructured chitosan-poly(vinyl alcohol) scaffolds: a biomimetic extracellular matrix as dermal substitute, Biomed. Mater. 7 (2012), https://doi.org/10.1088/1748-6041/7/4/045005.
[15] Ł. Kaniuk, U. Stachewicz, Development and advantages of biodegradable PHA polymers based on electrospun PHBV fibers for tissue engineering and other biomedical applications, ACS Biomater. Sci. Eng. 7 (2021) 5339–5362, https://doi.org/10.1021/acsbiomaterials.1c00757.
[16] D. Sundaramurthi, U.M. Krishnan, S. Sethuraman, Electrospun nanofibers as scaffolds for skin tissue engineering, Polym. Rev. 54 (2014) 348–376, https://doi.org/10.1080/15583724.2014.881374.
[17] L. Liverani, A. Liguori, P. Zezza, C. Gualandi, M. Toselli, A.R. Boccaccini, M. L. Focarete, Nanocomposite electrospun fibers of poly(ε-caprolactone)/bioactive glass with shape memory properties, Bioact. Mater. 11 (2022) 230–239, https://doi.org/10.1016/j.bioactmat.2021.09.020.
[18] B. Azimi, L. Thomas, A. Fusco, O.I. Kalaoglu-Altan, P. Basnett, P. Cinelli, K. de Clerck, I. Roy, G. Donnarumma, M.B. Coltelli, S. Danti, A. Lazzeri, Electrosprayed chitin nanofibril/electrospun polyhydroxyalkanoate fiber mesh as functional nonwoven for skin application, J. Funct. Biomater. 11 (2020), https://doi.org/10.3390/jfb11030062.
[19] R. Kurpanik, E. Stodolak-Zych, Chemical and physical modifications of electrospun fibers as a method to stimulate tissue regeneration - minireview, Eng. Biomater. 159 (2021) 31–41, https://doi.org/10.34821/eng.biomat.159.2021.31-41.
[20] S. Metwally, S. Ferraris, S. Spriano, Z.J. Krysiak, Ł. Kaniuk, M.M. Marzec, S.K. Kim, P.K. Szewczyk, A. Gruszczyński, M. Wytrwal-Sarna, J.E. Karbowniczek, A. Bernasik, S. Kar-Narayan, U. Stachewicz, Surface potential and roughness controlled cell adhesion and collagen formation in electrospun PCL fibers for bone regeneration, Mater. Des. 194 (2020), https://doi.org/10.1016/j.matdes.2020.108915.
[21] A. Ivanoska-Dacikj, U. Stachewicz, Smart textiles and wearable technologies-opportunities offered in the fight against pandemics in relation to current COVID-19 state, Rev. Adv. Mater. Sci. 59 (2020) 487–505, https://doi.org/10.1515/rams-2020-0048.
[22] G.A.R. Nobes, R.H. Marchessault, D. Maysinger, Polyhydroxyalkanoates: materials for delivery systems, Drug Deliv. 5 (1998) 167–177.
[23] H.C. Chang, T. Sun, N. Sultana, M.M. Lim, T.H. Khan, A.F. Ismail, Conductive PEDOT:PSS coated polylactide (PLA) and poly(3-hydroxybutyrate-co-3-hydroxyvalerate) (PHBV) electrospun membranes: fabrication and characterization, Mater. Sci. Eng. C 61 (2016) 396–410, https://doi.org/10.1016/j.msec.2015.12.074.
[24] Ł. Kaniuk, Z.J. Krysiak, S. Metwally, U. Stachewicz, Osteoblasts and fibroblasts attachment to poly(3-hydroxybutyric acid-co-3-hydrovaleric acid) (PHBV) film and electrospun scaffolds, Mater. Sci. Eng. C 110 (2020), https://doi.org/10.1016/j.msec.2020.110668.
[25] M. Avella, E. Martuscelli, M. Raimo, Review Properties of Blends and Composites Based on Poly(3-Hydroxy)butyrate (PHB) and Poly(3-Hydroxybutyrate-Hydroxyvalerate) (PHBV) Copolymers, n.d.
[26] Ł. Kaniuk, A. Podborska, U. Stachewicz, Enhanced mechanical performance and wettability of PHBV fiber blends with evening primrose oil for skin patches improving hydration and comfort, J. Mater. Chem. B 10 (2022) 1763–1774, https://doi.org/10.1039/D1TB02805G.
[27] K. Sudesh, H. Abe, Y. Doi, Synthesis, Structure and Properties of Polyhydroxyalkanoates: Biological Polyesters, n.d.
[28] M.B. Brown, S.A. Jones, Hyaluronic acid: a unique topical vehicle for the localized delivery of drugs to the skin, J. Eur. Acad. Dermatol. Venereol. 19 (2005) 308–318, https://doi.org/10.1111/j.1468-3083.2004.01180.x.
[29] J. Necas, L. Bartosikova, P. Brauner, J. Kolar, Hyaluronic Acid (Hyaluronan): a Review, 2008.
[30] M.E. Smithmyer, L.A. Sawicki, A.M. Kloxin, Hydrogel scaffolds as in vitro models to study fibroblast activation in wound healing and disease, Biomater. Sci. 2 (2014) 634–650, https://doi.org/10.1039/c3bm60319a.
[31] E. Ahmadian, S.M. Dizaj, A. Eftekhari, E. Dalir, P. Vahedi, A. Hasanzadeh, M. Samiei, The potential applications of hyaluronic acid hydrogels in biomedicine, Drug Res. 70 (2020) 6–11, https://doi.org/10.1055/a-0991-7585.
[32] J.M. Medina, A. Thomas, C.R. Denegar, Knee osteoarthritis: should your patient opt for hyaluronic acid injection? J. Fam. Pract. 55 (2006) 669–675.
[33] R. Barbucci, S. Lamponi, A. Borzacchiello, L. Ambrosio, M. Fini, P. Torricelli, R. Giardino, Hyaluronic Acid Hydrogel in the Treatment of Osteoarthritis, 2002.
[34] P. Boukamp, R.T. Petrussevska, D. Breitkreutz, J. Hornung, A. Markham, N. E. Fusenig, Normal keratinization in a spontaneously immortalized aneuploid human keratinocyte cell line, J. Cell Biol. 106 (1988) 761–771.
[35] I. Colombo, E. Sangiovanni, R. Maggio, C. Mattozzi, S. Zava, Y. Corbett, M. Fumagalli, C. Carlino, P.A. Corsetto, D. Scaccabarozzi, S. Calvieri, A. Gismondi, D. Taramelli, M. Dell'Agli, HaCaT cells as a reliable in vitro differentiation model to dissect the inflammatory/repair response of human keratinocytes, Mediat. Inflamm. (2017), https://doi.org/10.1155/2017/7435621, 2017.
[36] P.K. Szewczyk, U. Stachewicz, The impact of relative humidity on electrospun polymer fibers: from structural changes to fiber morphology, Adv. Colloid Interface Sci. 286 (2020), https://doi.org/10.1016/j.cis.2020.102315.
[37] K.A.G. Katsogiannis, G.T. Vladisavljević, S. Georgiadou, Porous electrospun polycaprolactone (PCL) fibres by phase separation, Eur. Polym. J. 69 (2015) 284–295, https://doi.org/10.1016/j.eurpolymj.2015.01.028.
[38] R.M. Nezarati, M.B. Eifert, E. Cosgriff-Hernandez, Effects of humidity and solution viscosity on electrospun fiber morphology, Tissue Eng. C Methods 19 (2013) 810–819, https://doi.org/10.1089/ten.tec.2012.0671.
[39] J.E. Karbowniczek, Ł. Kaniuk, K. Berniak, A. Gruszczyński, U. Stachewicz, Enhanced cells anchoring to electrospun hybrid scaffolds with PHBV and HA particles for bone tissue regeneration, Front. Bioeng. Biotechnol. 9 (2021), https://doi.org/10.3389/fbioe.2021.632029.
[40] A. Bianco, M. Calderone, I. Cacciotti, Electrospun PHBV/PEO co-solution blends: microstructure, thermal and mechanical properties, Mater. Sci. Eng. C 33 (2013) 1067–1077, https://doi.org/10.1016/j.msec.2012.11.030.

[41] J. Ding, J. Zhang, J. Li, D. Li, C. Xiao, H. Xiao, H. Yang, X. Zhuang, X. Chen, Electrospun polymer biomaterials, Prog. Polym. Sci. 90 (2019) 1–34, https://doi.org/10.1016/j.progpolymsci.2019.01.002.
[42] H. Cheng, X. Yang, X. Che, M. Yang, G. Zhai, Biomedical application and controlled drug release of electrospun fibrous materials, Mater. Sci. Eng. C 90 (2018) 750–763, https://doi.org/10.1016/j.msec.2018.05.007.
[43] M. Liu, X.P. Duan, Y.M. Li, D.P. Yang, Y.Z. Long, Electrospun nanofibers for wound healing, Mater. Sci. Eng. C 76 (2017) 1413–1423, https://doi.org/10.1016/j.msec.2017.03.034.
[44] C.A. Martínez-Pérez, Electrospinning: a promising technique for drug delivery systems, Rev. Adv. Mater. Sci. 59 (2020) 441–454, https://doi.org/10.1515/rams-2020-0041.
[45] M. van Beek, L. Jones, H. Sheardown, Hyaluronic acid containing hydrogels for the reduction of protein adsorption, Biomaterials 29 (2008) 780–789, https://doi.org/10.1016/j.biomaterials.2007.10.039.
[46] Z.J. Krysiak, M.Z. Gawlik, J. Knapczyk-Korczak, L. Kaniuk, U. Stachewicz, Hierarchical composite meshes of electrospun PS microfibers with PA6 nanofibers for regenerative medicine, Materials 13 (2020), https://doi.org/10.3390/MA13081974.
[47] P.K. Szewczyk, D.P. Ura, S. Metwally, J. Knapczyk-Korczak, M. Gajek, M. M. Marzec, A. Bernasik, U. Stachewicz, Roughness and fiber fraction dominated wetting of electrospun fiber-based porous meshes, Polymers 11 (2019), https://doi.org/10.3390/polym11010034.
[48] J. Knapczyk-Korczak, D.P. Ura, M. Gajek, M.M. Marzec, K. Berent, A. Bernasik, J. P. Chiverton, U. Stachewicz, Fiber-based composite meshes with controlled mechanical and wetting properties for water harvesting, ACS Appl. Mater. Interfaces 12 (2020) 1665–1676, https://doi.org/10.1021/acsami.9b19839.
[49] M. Dovedytis, Z.J. Liu, S. Bartlett, Hyaluronic acid and its biomedical applications: a review, Eng. Regen. 1 (2020) 102–113, https://doi.org/10.1016/j.engreg.2020.10.001.
[50] J.J. Ahire, D. Robertson, D.P. Neveling, A.J. van Reenen, L.M.T. Dicks, Hyaluronic acid-coated poly(d,l-lactide) (PDLLA) nanofibers prepared by electrospinning and coating, RSC Adv. 6 (2016) 34791–34796, https://doi.org/10.1039/c6ra01996j.
[51] K.N. How, W.H. Yap, C.L.H. Lim, B.H. Goh, Z.W. Lai, Hyaluronic acid-mediated drug delivery system targeting for inflammatory skin diseases: a mini review, Front. Pharmacol. 11 (2020), https://doi.org/10.3389/fphar.2020.01105.
[52] S.N. Gorodzha, A.R. Muslimov, D.S. Syromotina, A.S. Timin, N.Y. Tcvetkov, K. v. Lepik, A.v. Petrova, M.A. Surmeneva, D.A. Gorin, G.B. Sukhorukov, R. A. Surmenev, A comparison study between electrospun polycaprolactone and piezoelectric poly(3-hydroxybutyrate-co-3-hydroxyvalerate) scaffolds for bone tissue engineering, Colloids Surf. B Biointerfaces 160 (2017) 48–59, https://doi.org/10.1016/j.colsurfb.2017.09.004.
[53] M. Gadomska, K. Musiał, A. Sionkowska, New materials based on hyaluronic acid and egg albumin mixture, Eng. Biomater. 160 (2021) 15–21, https://doi.org/10.34821/eng.biomat.160.2021.15-21.
[54] B. Corradetti, F. Taraballi, J.O. Martinez, S. Minardi, N. Basu, G. Bauza, M. Evangelopoulos, S. Powell, C. Corbo, E. Tasciotti, Hyaluronic acid coatings as a simple and efficient approach to improve MSC homing toward the site of inflammation, Sci. Rep. 7 (2017), https://doi.org/10.1038/s41598-017-08687-3.
[55] R. Augustine, A. Hasan, N.K. Patan, Y.B. Dalvi, R. Varghese, A. Antony, R.N. Unni, N. Sandhyarani, A.E. al Moustafa, Cerium oxide nanoparticle incorporated electrospun poly(3-hydroxybutyrate-co-3-hydroxyvalerate) membranes for diabetic wound healing applications, ACS Biomater. Sci. Eng. 6 (2020) 58–70, https://doi.org/10.1021/acsbiomaterials.8b01352.
[56] U. Stachewicz, P.K. Szewczyk, A. Kruk, A.H. Barber, A. Czyrska-Filemonowicz, Pore shape and size dependence on cell growth into electrospun fiber scaffolds for tissue engineering: 2D and 3D analyses using SEM and FIB-SEM tomography, Mater. Sci. Eng. C 95 (2019) 397–408, https://doi.org/10.1016/j.msec.2017.08.076.
[57] T.-T. Sun, H. Green, Differentiation of the epidermal keratinocyte in cell culture : formation of the cornified envelope, Cell 9 (1976) 511–521.
[58] Y. Barrandon, H. Green, Cell size as a determinant of the clone-forming ability of human keratinocytes, Cell Biol. 82 (1985) 5390–5394.
[59] U. Stachewicz, T. Qiao, S.C.F. Rawlinson, F.V. Almeida, W.Q. Li, M. Cattell, A. H. Barber, 3D imaging of cell interactions with electrospun PLGA nanofiber membranes for bone regeneration, Acta Biomater. 27 (2015) 88–100, https://doi.org/10.1016/j.actbio.2015.09.003.
[60] X.T. Li, Y. Zhang, G.Q. Chen, Nanofibrous polyhydroxyalkanoate matrices as cell growth supporting materials, Biomaterials 29 (2008) 3720–3728, https://doi.org/10.1016/j.biomaterials.2008.06.004.
[61] I. Unalan, S.J. Endlein, B. Slavik, A. Buettner, W.H. Goldmann, R. Detsch, A. R. Boccaccini, Evaluation of electrospun poly(ε-caprolactone)/gelatin nanofiber mats containing clove essential oil for antibacterial wound dressing, Pharmaceutics 11 (2019), https://doi.org/10.3390/pharmaceutics11110570.
[62] T. Léguillier, M. Lecsö Bornet, C. Lémus, D. Rousseau-Ralliard, N. Lebouvier, E. Hnawia, M. Nour, W. Aalbersberg, K. Ghazi, P. Raharivelomanana, P. Rat, The wound healing and antibacterial activity of five ethnomedical Calophyllum inophyllum oils: an alternative therapeutic strategy to treat infected wounds, PLoS One 10 (2015), https://doi.org/10.1371/journal.pone.0138602.
[63] N. Goonoo, F. Gimié, I. Ait-Arsa, C. Cordonin, J. Andries, D. Jhurry, A. Bhaw-Luximon, Piezoelectric core-shell PHBV/PDX blend scaffolds for reduced superficial wound contraction and scarless tissue regeneration, Biomater. Sci. 9 (2021) 5259–5274, https://doi.org/10.1039/d1bm00379h.
[64] J. Voigt, V.R. Driver, Hyaluronic acid and wound healing, Wound Repair Regen. 20 (2012) 317–331, https://doi.org/10.1111/j.1524-475X.2012.00777.x.
[65] J. Elisseeff, Injectable cartilage tissue engineering, Expet Opin. Biol. Ther. 4 (2004) 1849–1859, https://doi.org/10.1517/14712598.4.12.1849.
[66] C. Chung, I.E. Erickson, R.L. Mauck, J.A. Burdick, Differential behavior of auricular and articular chondrocytes in hyaluronic acid hydrogels, Tissue Eng. 14 (2008) 1121–1131, https://doi.org/10.1089/ten.tea.2007.0291.
[67] W.Y.J. Chen, G. Abatangelo, Functions of Hyaluronan in Wound Repair, Wound Repair and Regenaration, 1999, pp. 79–89. March-April.
[68] J.v. Gruber, R. Holtz, J. Riemer, Hyaluronic acid (HA) stimulates the in vitro expression of CD44 proteins but not HAS1 proteins in normal human epidermal keratinocytes (NHEKs) and is HA molecular weight dependent, J. Cosmet. Dermatol. 21 (2022) 1193–1198, https://doi.org/10.1111/jocd.14188.
[69] T. Murakami, S. Otsuki, Y. Okamoto, K. Nakagawa, H. Wakama, N. Okuno, M. Neo, Hyaluronic acid promotes proliferation and migration of human meniscus cells via a CD44-dependent mechanism, Connect. Tissue Res. 60 (2019) 117–127, https://doi.org/10.1080/03008207.2018.1465053.